SENSITIVITY OF BELLHOP INTENSITY TO UNCERTAINTY IN SOUND SPEED

Diana McCammon *[1] **and Sean Pecknold** †[2]
[1]McCammon Acoustical Consulting, Black Rock, NS and Maritime Way Scientific, Ottawa, ON
[2]DRDC Atlantic Research Centre, Dartmouth, NS

1 Introduction

The Bellhop Gaussian beam solution formulated by Porter and Bucker [1] for acoustic propagation in an underwater environment is a complicated function of the environmental sound speed. In addition to the standard set of ray tracing differential equations, the incoherent intensity from the Bellhop algorithm is dependent upon a beamwidth factor obtained by the integration of a second pair of differential equations along the ray path. This factor can be expressed in closed form for linear constant gradient sound speed profiles. The derivatives of these equations with respect to (w.r.t) the sound speed in each layer express the sensitivity of the Gaussian Beam method to uncertainty in sound speed. Using these derivatives, the uncertainty in the transmission loss can be estimated from the uncertainty in the environment. In this paper, we present a pictorial display of the Bellhop intensity derivatives w.r.t. the sound speed.

2 Method

The Bellhop Gaussian Beam incoherent intensity can be written as

$$I(r,z) = \sum A \,\frac{c}{c_0}\, \frac{\exp(\frac{-n^2}{2q^2})}{q}\, \mathfrak{R}_B^2 \mathfrak{R}_S^2 \qquad (1)$$

where A is a constant, independent of beam number, that carries the cylindrical spreading and attenuation. The symbols $\mathfrak{R}$ contain the reflections coefficients from the boundaries (bottom and surface) and c is the sound speed The Gaussian factor depends upon n, the normal distance from the ray's position to the receiver location, and the beam's width q. The value of q satisfies the second system of differential equations that Bellhop traces and is capped when small. The function q is therefore an extremely important term in the amplitude of Bellhop.

When the sound speed layers are assumed to be linear with constant gradients, a closed-form expression can be found for q that is inversely proportional to the sine of the ray angle and the gradient of the layer. The function q can be differentiated with respect to the sound speed c in each layer, and therefore the intensity derivative dI/dc can be derived. It is found that one of the terms in this function is inversely proportional to $\sin^3\theta$, meaning that the sensitivity to the sound speed will be greatest as the beam is approaching a turning point.

The relation between the variance of the intensity σ_I^2 and the variance of the random sound speed uncertainty σ_c^2 is given in Papoulis [2] as

$$\sigma_I^2 = \left(\frac{dI}{dc}\right)^2 \sigma_c^2 \qquad (2)$$

This paper shows examples of the intensity derivatives' spatial distribution which highlight the regions where the uncertainty in sound speed would produce the highest uncertainty in the propagated intensity.

3 Results

3.1 Test environment

The sound speed profile used for these tests is shown in Fig 1. It is designed to provide structure to the acoustic field with both ducted and deep refracted rays. It features a surface duct as well as a sub-surface duct to illustrate the intensity and its derivative captured in each segment. The bottom is flat at 200m and the composition is hard sand to give good reflections. The frequency is 1000Hz, and about 400 beams are traced. The lowest SSP point, is defined well below the bottom depth.

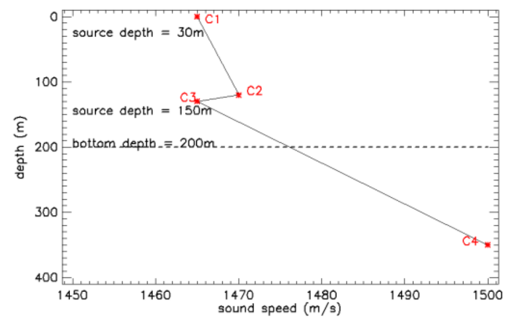

Figure 1 Sound speed profile defined by 4 points, c_1 thru c_4.

3.2 30 m source depth

The transmission loss at 1000Hz is shown in Fig 2 and reveals the expected ray concentrations in the surface duct as well as a pair of deep refracted rays and some leakage from the surface duct.

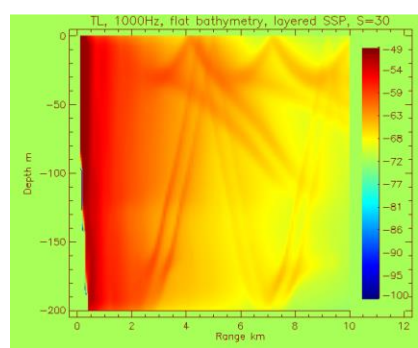

Figure 2 Full field transmission loss for 30m source.

Some of the dB intensity derivatives are shown in Fig 3. The upper plot is the derivative w.r.t. the surficial sound speed dI/dc_1. This plot is substantially the same for the derivative w.r.t. the second sound speed point dI/dc_2 (therefore not repeated here). The lower plot is the derivative w.r.t. c_3 and this plot is also substantially the same for the last SSP point dI/dc_4 (not shown here).

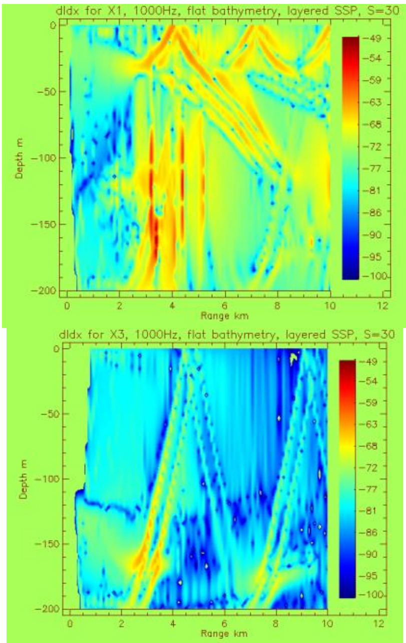

Figure 3 Full field intensity derivatives w.r.t. c_1 or c_2 (upper), c_3 or c_4 (lower).

3.3 150 m source depth

The transmission loss at 1000Hz for a 150m source (Fig. 4) shows the influence of the sub-surface duct as well as deeply cycled rays.

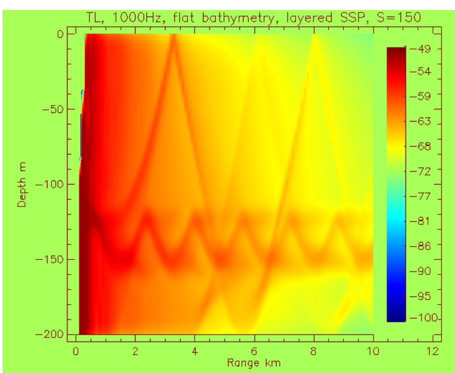

Figure 4 Full field transmission loss for 150m source.

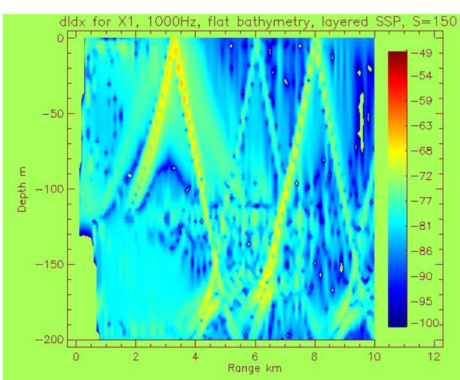

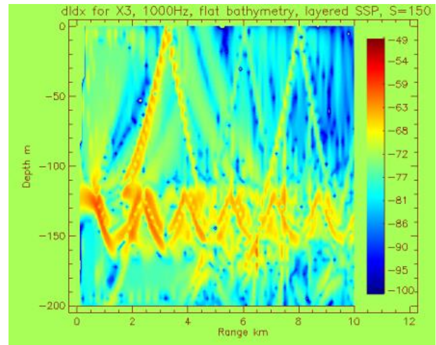

Figure 5 Full field intensity derivative w.r.t. c_1 or c_4 (bottom, previous column), c_2 or c_3 (above).

Some of the dB intensity derivatives are shown in Fig 5. The plot on the bottom of the previous column is the derivative w.r.t. the surficial sound speed dI/dc_1. This plot is substantially the same for the last sound speed point dI/dc_4 (not shown here). The plot above is the derivative w.r.t. c_3 and this plot is also substantially the same for the second SSP point dI/dc_2 (not shown here).

4 Discussion

A comparison of Fig 3 with Fig 2 and Fig 5 with Fig 4 shows that the intensity derivatives are largest along the edges of strong propagation intensity, particularly along caustic lines when the randomness is in the speeds defining the duct containing the source. The sound ducts that support strong propagation are also highly sensitive to changes in these speeds. The first set of intensity derivative plots (Fig 3) show strong sensitivity in dI/dc_1 and dI/dc_2 which define the surface duct in which the source is located, with much lower contributions from randomness in c_3 and c_4 because they lie outside the surface duct. Similarly, the second set of intensity derivative plots (Fig 5) show strong contributions from the derivative of the intensity w.r.t. c_2 and c_3 which define the sub-surface duct in which the source is located, but not as much sensitivity in dI/dc_1 or dI/dc_4. When the speed uncertainty is in the sound speed points outside the duct, only the deep cycled rays are affected.

5 Conclusion

Given the relationship between the variance of the intensity and the variance of the underlying sound speeds shown in Eq 2, the implication is that obtaining an accurate estimate for the speeds surrounding the source depth will be of most benefit in reducing the uncertainty in predicted transmission loss.

References

[1] M. Porter and H. Bucker Gaussian beam tracing for computing ocean acoustic fields, *J. Acoust Soc. Am*. 82 (4):1349, 1987.

[2] A. Papoulis, Probability, Random Variables, and Stochastic Processes, 2nd edition McGraw-Hill, 1984